# Nitrogen Metabolism in *Methanobacterium thermoautotrophicum*: A Solution and Solid-State $^{15}N$ NMR Study†

Byong-Seok Choi,‡ James E. Roberts,§,‖ Jeremy N. S. Evans,‡ and Mary F. Roberts*,‡

*Department of Chemistry and Francis Bitter National Magnet Laboratory, Massachusetts Institute of Technology, Cambridge, Massachusetts 02139*

*Received August 27, 1985; Revised Manuscript Received December 2, 1985*

ABSTRACT: Nitrogen metabolism in *Methanobacterium thermoautotrophicum* has been studied with high-resolution and solid-state $^{15}N$ NMR spectroscopy. The time course for $^{15}NH_4Cl$ uptake and distribution among small molecules shows several key amino acids whose relative ratios vary dramatically with cell growth. In log-phase growth, the majority of $^{15}N$ label is incorporated into glutamate, while alanine and arginine are also labeled but to a much lesser extent. As cells enter the stationary phase, relative glutamate levels decrease and alanine becomes the dominant $^{15}N$ pool. When cells become nitrogen starved, the original pattern reappears. An examination of $^{15}N$ incorporation into arginine and arginine-like material purified from cell extracts shows that the $\alpha$-amino nitrogen is removed, while the $^{15}N$-labeled guanidino group remains intact. This implies that a transaminase activity is responsible for the catabolism of arginine. Cross-polarization magic angle sample spinning NMR spectra of cell debris and partially purified cell walls show that $^{15}N$ label is incorporated primarily into amide nitrogens.

Methanogens are anaerobes with unique biochemistry: they use molecular $H_2$ to reduce $CO_2$ to $CH_4$ (Zeikus, 1977; Daniels et al., 1984). This reaction is coupled to the production of cellular ATP. They have a variety of unusual cofactors, possess ether-linked lipids, and have pseudomurein cell walls. $CO_2$ is the sole carbon source for these organisms and is assimilated into cell carbon as well as being reduced to $CH_4$ (Fuchs et al., 1978; Stupperich & Fuchs, 1981). Nitrogen assimilation can occur exclusively from $NH_4^+$ (i.e., $NH_4Cl$). The only information available on nitrogen metabolism in *Methanobacterium thermoautotrophicum* has been deduced indirectly from assays of cell extracts for specific enzymatic activities or from short-lived radioactive $^{13}N$ tracer studies (Kenealy et al., 1982). Given the unusual reactions in *M. thermoautotrophicum*, it is possible that nitrogen assimilation will also differ from other anaerobic organisms.

A promising technique for studying metabolism in cells is NMR spectroscopy. Specific label uptake and distribution and unusual metabolites or pathways can be monitored. As an example of the latter, 2,3-cyclopyrophosphoglycerate, the major soluble phosphate compound in *M. thermoautotrophicum* (Kanodia & Roberts, 1983; Seeley & Fahrney, 1983), was first detected in vivo by $^{31}P$ NMR spectroscopy. For the study of nitrogen metabolism, $^{15}N$ NMR offers several advantages. The $^{15}N$ chemical shift range is large ($\sim$900 ppm), and each type of nitrogen has a characteristic chemical shift. The natural abundance of $^{15}N$ is low (0.37%), which ensures that resonances observed in an $^{15}N$-enriched feedng experiment reflect specific label uptake and metabolism. A number of organisms have been studied in detail with high-resolution and solid-state $^{15}N$ NMR spectroscopy, for example, *Neurospora crassa* (Jacob et al., 1980; Legerton et al., 1981; Kanamori et al., 1982), soybean leaves (Schaefer et al., 1981a,b) *Brevibacterium lactofermentum* (Haran et al., 1983), and bacterial cell wall components (Lapidot & Irving, 1977, 1979; Jacob et al., 1985). In this work we have used $^{15}N$ NMR spectroscopy to follow the metabolism of $^{15}NH_4Cl$ by *M. thermoautotrophicum*. High-resolution $^{15}N$ NMR studies of ethanol extracts give a direct measurement of total nitrogen flux into soluble metabolites. They have allowed us to establish (i) the glutamate synthase/glutamine synthetase (or glutamate dehydrogenase) pathway for ammonia assimilation, (ii) the glutamate-alanine transaminase pathway as a way of supplying nitrogen for glutamate synthesis in stationary phase cells, and (iii) an arginine catabolic pathway involving arginine transamination as the first step. CP-MASS[1] NMR spectra comparing purified cell wall with insoluble cell debris are consistent with a pseudomurein structure in which most of the lysine residues are cross-linked.

## Materials and Methods

*Chemicals.* $^{15}N$-Labeled ammonium chloride (99% $^{15}N$) was purchased either from Stohler Isotopes (Waltham, MA) or from Cambridge Isotopes (Cambridge, MA). Amberlite IRA-400 ($OH^-$) resin was obtained from Aldrich (Milwaukee, WI); $\gamma$-guanidinobutyric acid, sodium pyruvate, and glutamate-pyruvate transaminase were obtained from Sigma (St. Lous, MO); $CO_2/H_2$ (1:4 v/v) was obtained unanalyzed from Matheson Gas (Gloucester, MA). All other chemicals were reagent-grade.

*Cell Growth.* *M. thermoautotrophicum* $\Delta$H cells were grown in a 2-L Applikon fermenter under conditions described previously (Evans et al., 1985). The medium contained 40 mM $^{14}NH_4Cl$, 10 mM inorganic phosphate, and 50 mM PIPES, pH 7.1 (at room temperature). Cultures were grown at 62 °C under continuous purging of $H_2/CO_2$ (flow rate = 210 cm$^3$ min$^{-1}$ at 12 psi) and $H_2S$ (flow rate = 0.8 cm$^3$ min$^{-1}$

† This work was supported by the Basic Research Department of The Gas Research Institute (Contract 5083-260-0867).

* Author to whom correspondence should be addressed.

‡ Department of Chemistry.

§ Francis Bitter National Magnet Laboratory.

‖ Present address: Department of Chemistry, Lehigh University, Bethlehem, PA 18015.

[1] Abbreviations: CP-MASS, cross-polarization magic angle sample spinning; NOE, nuclear Overhauser effect; PIPES, 1,4-piperazinediethanesulfonic acid; HPLC, high-pressure liquid chromatography.

0006-2960/86/0425-2243$01.50/0 

at 12 psi). When the culture reached an $OD_{660} \sim 1$ (measured in a Turner Model 330 spectrophotometer), $^{15}NH_4Cl$ was added anaerobically to a final concentration of 20 mM. Aliquots of cells were removed subsequently from the fermenter as a function of time, cooled, and rapidly harvested by centrifugation (8000*g*, 30 min). Cell pellets were washed twice with buffer (50 mM PIPES, 10 mM EDTA, pH 7.1) and centrifuged again (8000*g*, 30 min).

*Cell Extracts.* Cell extracts for high-resolution $^{15}N$ NMR studies and amino acid analysis were made according to previously described procedures (Evans et al., 1985). The particulate cell residues from these extracts were dried by lyophilization and used for cell wall purification or for study by CP-MASS NMR spectroscopy.

*Amino Acid Analysis.* The total free amino acid content of ethanol extracts of *M. thermoautotrophicum* harvested as a function of time was determined with a Glenco MM-60 amino acid analyzer.

*Purification of [$^{15}N$]Arginine from Cell Extracts.* Arginine was purified from other amino acids in cell extracts by the method of Winters and Kunin (1949). Each sample (2 mL) was applied to a column (0.95 × 8 cm) of IRA-400 ($OH^-$) ion-exchange resin equilibrated with deionized water. Three column volumes of water was used to elute the arginine and similar basic material. The eluant was lyophilized for subsequent NMR analysis.

*Purification of Cell Walls.* Cell walls were purified according to the method of Jacob et al. (1983). Cell debris from extracts was washed 4 times with doubly deionized water, suspended in 50 mL of 0.1 M potassium phosphate, pH 8.0, containing 0.1% (w/v) trypsin (Sigma) and 1 mg of deoxyribonuclease (Sigma), and shaken at 37 °C for 18 h. The digest was centrifuged (25000*g*, 25 min), and the cell wall sediment was washed 4 times with doubly deionized water. This particulate fraction was lyophilized and used for CP-MASS NMR analysis.

*$^{15}N$ NMR Spectroscopy.* High-resolution $^{15}N$ NMR experiments in 10-mm NMR tubes were performed on a 9.4 T Bruker AM-400 spectrometer (Tufts University Medical School) operating at 40.55 MHz. Proton-decoupled $^{15}N$ NMR spectra were obtained by gated $^1H$ decoupling with full nuclear Overhauser effect (NOE), a pulse width (90°) of 22.2 μs, 20-kHz spectral width, 2.4-Hz digital resolution (16K data points), and a recycle time of 15 s. Although NOEs for $^{15}N$ in small molecules are negative, we have plotted the spectra so that the peaks are positive. The free induction decays were exponentially multiplied with a line broadening of 10 Hz prior to Fourier transformation. These optimal NMR conditions did not result in saturation of any of the resonance except $NH_4^+$ (i.e., recycle time $\gg T_1$ and $T_2$) or in differential NOE's (determined by integrating resonances obtained under conditions of gated $^1H$ decoupling without maintenance of NOE). Dry samples obtained as described above were dissolved in buffer (50 mM sodium phosphate, 10 mM EDTA, pH 7.0, 6% $D_2O$). $Na^{15}NO_3$ (10 mM) was added to each sample to serve as an internal chemical shift reference and intensity standard. Chemical shifts were estimated to within an accuracy of 0.05 ppm.

CP-MASS NMR spectra were obtained on a home-built pulse spectrometer operating at 317.7 MHz for $^1H$ and 32.2 MHz for $^{15}N$ (Francis Bitter National Magnet Laboratory, MIT). The maximum radio-frequency field strengths were approximately 65 G for $^{15}N$ and 25 G for $^1H$. Powdered samples of 100–200 mg were tightly packed into ceramic double-bearing rotors (Doty Scientific), and sample spinning

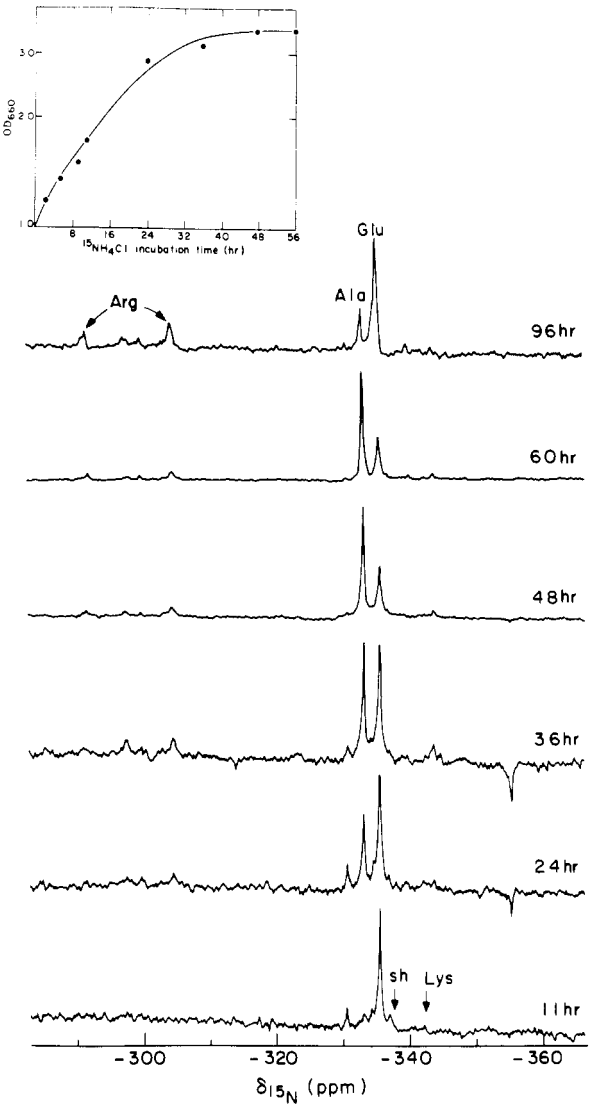


FIGURE 1: $^1H$-decoupled 40.5-MHz $^{15}N$ NMR spectra of ethanol extracts of *M. thermoautotrophicum* cells incubated with $^{15}NH_4Cl$ for the times indicated. The 11-h spectrum is for log-phase cells; 24 and 36 h represent early stationary phase cell; 48 and 60 h represent stationary-phase cells; at 96 h the cells are under nitrogen-starvation conditions. The 11-h spectrum was obtained wtih 10000 transients, and the other time points were obtained with 5000 transients. (Inset) Growth curve of *M. thermoautotrophicum* during the course of the $^{15}NH_4Cl$ incubation.

rates varied from 3.36 to 3.45 kHz. Typical cross-polarization contact times were 1.5 ms with 5-s recycle delays between scans. $^{15}N$ chemical shifts of solid samples were referenced to external solid $^{15}NH_4Cl$ (99% $^{15}N$).

## RESULTS

*$^{15}N$ NMR Spectra of Soluble Cell Extracts.* An extract of *M. thermoautotrophicum* cells harvested after 11 h of growth in media containing $^{15}NH_4Cl$ gave rise to the $^{15}N$ NMR spectrum shown in Figure 1. Most of these resonances can be assigned by comparing the observed chemical shifts with published values for amino acids and nucleotides (Legerton et al., 1981; Haran et al., 1983). The resonances observed arise from the α-amino nitrogen of alanine (−333 ppm) and the α-amino nitrogens of glutamate, lysine, and arginine (all overlapping at ca. −335 ppm). The side-chain nitrogens of arginine (−291 and −304 ppm) are not detectable at early time points. The peak at −354.5 ppm arises from ammonium ions. There is an additional resonance at −330 ppm, assigned to residual PIPES from the growth medium and subsequent cell

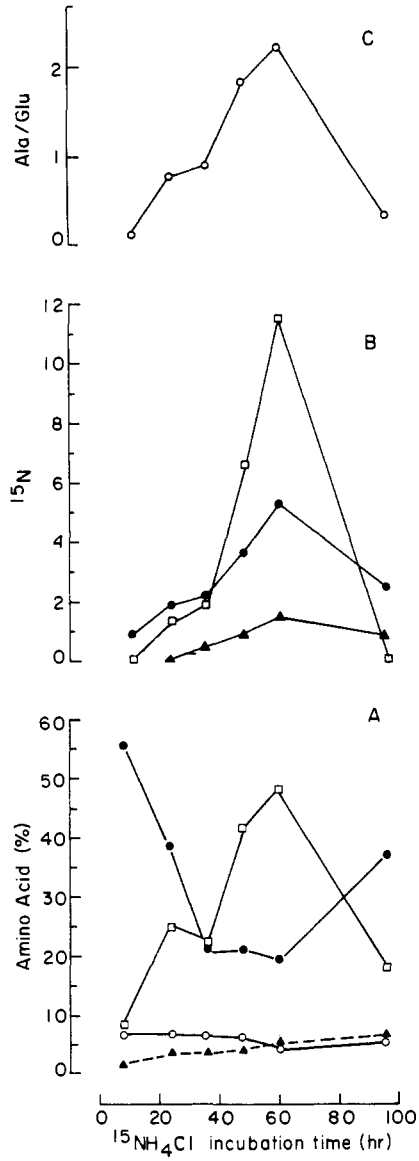


FIGURE 2: Kinetics of $^{15}NH_4Cl$ uptake and labeling of specific amino acids by *M. thermoautotrophicum*. The amino acid analyses were determined by HPLC of acid-hydrolyzed ethanol extracts. (A) Total percent amino acid as a function of time: Ala (□), Glu (●), Asp (○), and Arg (▲). (B) Relative $^{15}N$ intensities for Ala (□), Glu (●) (which also includes a small contribution from the $\alpha$-$NH_2$ of aspartate, lysine, and arginine), and Arg side-chain nitrogens (▲). (C) Ratio of $^{15}N$ incorporation into Ala compared to Glu as a function of growth time.

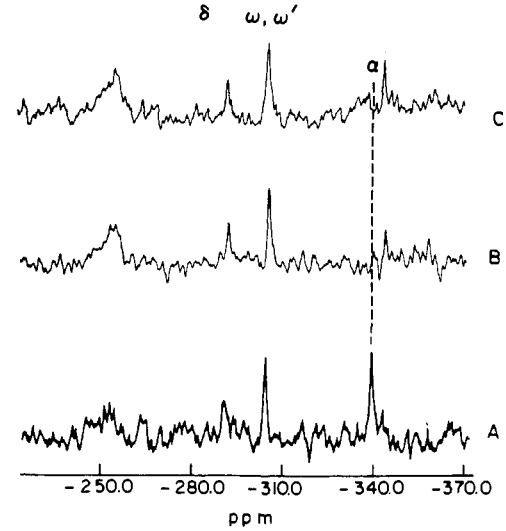


FIGURE 3: $^1H$-decoupled 40.5-MHz $^{15}N$ NMR spectra of [$^{15}N$]arginine and related basic compounds (pH 8.8) purified from extracts of *M. thermoautotrophicum* fed with $^{15}NH_4Cl$ and harvested after (A) 22 h (late log-phase cells), (B) 36 h (early stationary phase cells), and (C) 60 h (stationary-phase cells). Spectra were obtained with 6000–8000 transients.

washes. Figure 1 also shows NMR spectra of additional time points up to 96 h of growth with $^{15}NH_4Cl$. A number of changes occur with time, notably the marked increase in intensity of the $\alpha$-$NH_2$ alanine resonance (−333 ppm) and the decrease in intensity for the resonance assigned to the $\alpha$-$NH_2$ of glutamate, lysine, and arginine (−335 ppm). The distinct unassigned shoulder on the large resonance at −335 ppm is observed at early time points but not detected in the 48-h spectrum or subsequent time points.

For comparison with the NMR data, the growth curve of *M. thermoautotrophicum* under these experimental conditions is shown as an inset in Figure 1. During log-phase growth, the majority of $^{15}N$ is assimilated into the resonance representing the $\alpha$-$NH_2$ of glutamate and lysine (−335 ppm). The switch to alanine as the major labeled species occurs when the cells reach stationary phase. Under nitrogen starvation conditions (96-h sample), the amino acid labeling pattern reverses from alanine abundance to glutamate abundance.

*Total Amino Acid Analysis.* The $^{15}N$ NMR data on specifically labeled amino acid pools were supplemented with cation-exchange HPLC amino acid analyses to determine total free amino acid pools. The results of this are summarized in Figure 2. Glutamate is the most abundant amino acid at early time points (8 h). The distribution of intensities of the $^{15}N$ signals (Figure 2B) correlates well with the total amino acid content in the hydrolysates (Figure 2A). Thus, the resonance at −335 ppm can be identified as predominantly glutamate with smaller amounts of arginine and lysine $\alpha$-amino nitrogens contributing to its intensity. This was confirmed when an extract was treated with glutamate-pyruvate transaminase and pyruvate. The alanine resonance increased in intensity, and the resonance at −335 ppm was reduced by 70%. The most notable feature of the amino acid analyses is the rapid increase in the alanine pool at later time points. Glutamate initially decreases and then increases again upon nitrogen starvation. From the $^{15}N$ NMR data, alanine exhibits high $^{15}N$ labeling in stationary-phase cells while the glutamate $^{15}N$ labeling also increases, but not as dramatically. The ratio of specific $^{15}N$ uptake in alanine compared to glutamate is shown in Figure 2C. $^{15}N$ label incorporation into guanidino groups (i.e., arginine and closely related derivatives) is low and roughly constant.

*$^{15}N$ Labeling of Arginine.* The signals from the $N_\delta$ and $N_{\omega,\omega'}$ of arginine are observable after 24 h (see Figure 1), but the $\alpha$-amino signal cannot be detected because of overlap with other amino acids (primarily glutamate). To compare the extent of labeling between the guanidino and $\alpha$-amino nitrogens, arginine was separated from other amino acids by ion-exchange chromatography. Figure 3 shows $^{15}N$ NMR spectra of this purified arginine fraction from three different growth times. The resonance from the $\alpha$-amino nitrogen is clearly visible (−339 ppm at pH 8.8) during the late log phase growth (e.g., 22 h) but is greatly reduced in intensity at later growth times (36 and 60 h), while the $\omega,\omega'$ and $\delta$ nitrogens are labeled at all three time points. No new sharp $^{15}N$ peaks appear in the spectra of later time points. The resonances at around −250 and −343 ppm vary little in intensity and also do not shift with pH (in the range 7–12), so they probably represent other basic components of the cell cytoplasm. The loss of the $\alpha$-$NH_2$ of arginine can be explained if the catabolism in *M. thermoau-*

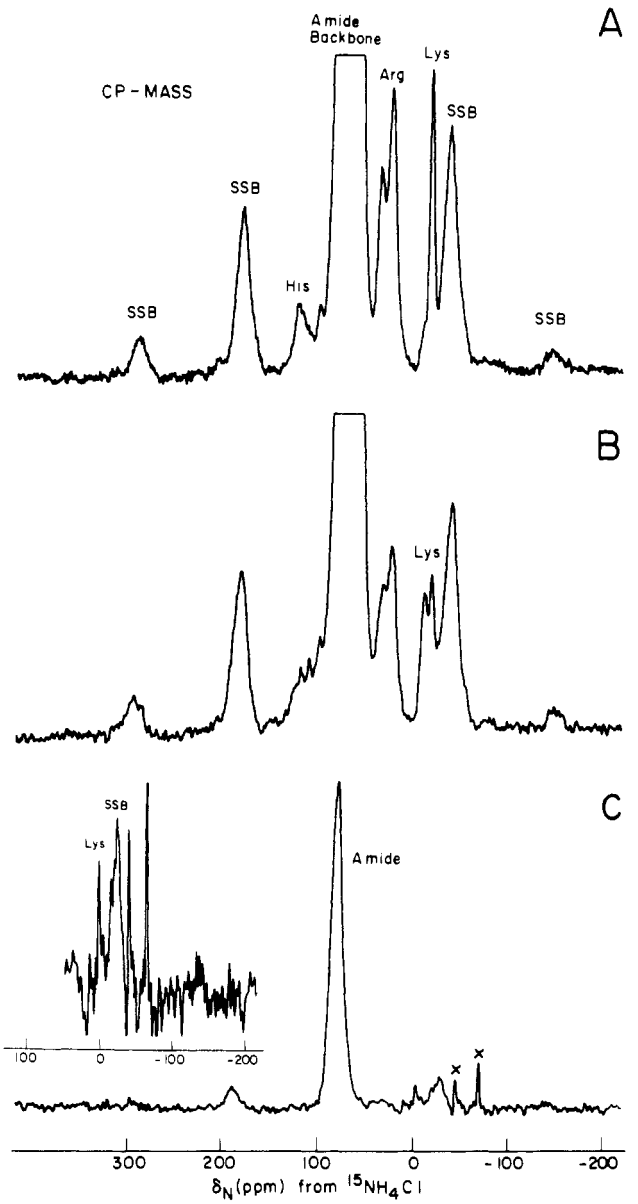


FIGURE 4: CP-MASS $^{15}N$ NMR (32.2-MHz) spectra of lyophilized particulate fractions of *M. thermoautotrophicum* grown with $^{15}NH_4Cl$ for 17 h: (A) total solid residue; (B) residue partially digested by trypsin and DNase; (C) completely digested sample of (A). Resonances are referenced to $^{15}NH_4Cl$, and identifications are indicated; SSB = spinning (or rotational) sideband; x = instrumental artifact.

*totrophicum* is different from those microorganisms that first remove or modify the guanidino group of arginine in their catabolic pathways. Since no other sharp, pH-dependent $^{15}N$ resonances are observed in the spectra at later time points, arginine catabolism in *M. thermoautotrophicum* must be initiated by transamination. The natural abundance $^{15}N$ NMR spectrum of $\gamma$-guanidinobutyrate, a product of such a catabolic scheme, shows $\delta$ and $\omega,\omega'$ nitrogens whose chemical shifts are identical with those of arginine.

*$^{15}N$ NMR Spectra of Particulate Samples (CP-MASS).* In order to detect incorporation of $^{15}N$ into proteins, cell wall, and nucleic acids, CP-MASS solid-state $^{15}N$ NMR spectroscopy was employed. Figure 4A shows a spectrum of cell debris after an ethanol extraction from cells grown for 36 h on $^{15}NH_4Cl$. There is a large resonance assignable to the amide backbone of protein and cell wall components. Large rotational (or spinning) sidebands flank this resonance; these are related to the residual chemical shift anisotropy of amide nitrogens. Resonances identified as the guanidino nitrogens

Scheme I: Assimilation of $NH_4^+$ into Various Nitrogenous Compounds in *M. thermoautotrophicum*[a]

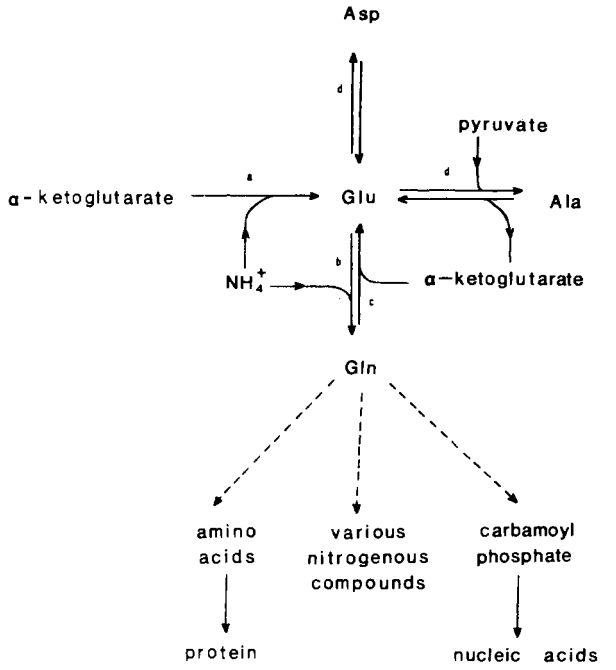


[a] Enzyme activities are as follows: a, glutamate dehydrogenase; b, glutamine synthetase; c, glutamate synthase; d, transaminase. The ultimate fate of nitrogen labels is also indicated by dashed lines.

of arginine, the $\epsilon$-amino of lysine, and the histidine ring nitrogens are also observed. The arginine and histidine peaks are incorporated into proteins, while lysine is present in the cell wall as well. This CP-MASS spectral pattern is more or less unchanged for 17–96 h of growth on $^{15}NH_4Cl$ (although the intensity increases for longer incubation times).

*M. thermoautotrophicum* possesses a pseudomurein cell wall (Kandler, 1974; König & Kandler, 1979a,b). To examine $^{15}N$ incorporation into the cell wall, the CP-MASS spectra of cell debris after treatment with trypsin and DNase were obtained (Figure 4B,C). Partial digestion results in a decrease in total $^{15}N$ intensity and a more pronounced decrease in intensity of side-chain nitrogens (Figure 4B). In the region for free amino groups, two resonances now appear (0 and −6 ppm), consistent with the $\alpha$-amino group of insoluble peptides and the $\epsilon$-amino group of lysine. After complete trypsin and DNase digestion (80% decrease in initial $^{15}N$ intensity), there is a complete loss of $^{15}N$ intensity for the arginine guanidino and histidine ring nitrogens (Figure 4C). Aside from the large amide resonance (and its rotational sidebands), there is a small sharp resonance at 0 ppm from solid $NH_4Cl$, the position for the $\alpha$-amino group of lysine in the cell wall. This is consistent with a pseudomurein structure in which the primary linkage for lysine involves the $\epsilon$-amino group and some degree of cross-linking that involves the $\alpha$-amino group.

## Discussion

While archaebacteria have a number of unusual carbon assimilation features (Evans et al., 1985; Stupperich et al., 1984; Taylor et al., 1976; Zeikus et al., 1977), the nitrogen metabolism appears relatively standard except for arginine catabolism. Key steps in nitrogen assimilation are shown in Scheme I. In actively growing cells, glutamate is the key amino acid. It can be the initial product of $NH_4^+$ fixation via glutamate dehydrogenase (a) or used to fix $NH_4^+$ into glutamine via glutamine synthetase (b). Glutamine is the nitrogen donor for a variety of compounds and can be converted back to glutamate via glutamate synthase (c). Transaminase activities can transfer the $\alpha$-$NH_2$ of glutamate to other amino

Scheme II: Initial Steps of Four Possible Catabolic Pathways for Arginine[a]

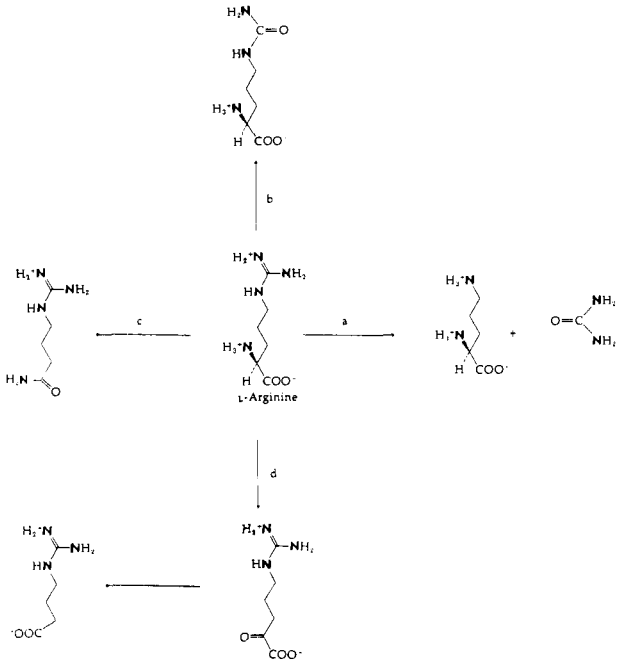


[a] a, arginase; b, arginine dihydrolase; c, hydroxylase; d, transaminase. The distribution of nitrogen label, originally uniform in arginine, is emphasized in each of the catabolic species.

acids (d). Our $^{15}N$ NMR results, which show high concentrations of glutamate, are consistent with this general scheme and previous short-term radioactive $^{13}N$-labeling studies of *M. thermoautotrophicum* (Kenealy et al., 1982). Similar ammonia-assimilating systems have been detected in many organisms, including *Cyanobacterium* (Meeks et al., 1978), *Escherichia coli* (Tyler, 1978), and *Alnus glutinosa* (Schubert et al., 1981). $^{15}N$ CP-MASS spectra of the insoluble cell residue obtained for different growth times on $^{15}NH_4Cl$ showed almost identical patterns consistent with protein biosynthesis as the major end product of nitrogen assimilation. A comparison of spectra for initial cell debris and fractionated cell wall indicates that incorporation of nitrogen into pseudomurein cell wall represents 20% of the total $^{15}N$ incorporation into insoluble material of *M. thermoautotrophicum*.

One of the interesting findings of the present high-resolution $^{15}N$ NMR work is that relative glutamate levels decrease and alanine becomes the dominant soluble $^{15}N$ pool as cells enter stationary phase. Unlike glutamine or glutamate, alanine is not a precursor to any known metabolite in *M. thermoautotrophicum*, and beyond its role in protein and cell wall synthesis, little is known about the physiological function of the large free alanine pool. Under conditions of ammonia deficiency, glutamic acid is formed from alanine by the alanine transaminase pathway (Scheme I). The metabolic switch observed here can be explained in the following way. The carbon backbone of L-alanine is formed from pyruvate, a compound produced early in the carbon assimilation chain, and is a key component of both protein and the pseudomurein cell wall of *M. thermoautotrophicum*. Unlike Gram-negative bacteria that possess murein cell walls with D-alanine, methanobacteria use L-alanine (Hammes et al., 1979). Thus, if there is no drain on the alanine pool for cell wall synthesis, but only for protein synthesis, alanine will accumulate. Because the nitrogen of alanine can be converted to the nitrogen of glutamate with release of pyruvate, alanine may also be a convenient reservoir of both the amino groups and pyruvate made during nitrogen and carbon sufficiency. The glutamate-alanine transaminase pathway can be used to supply nitrogen for glutamic acid synthesis. The $^{15}N$ NMR profiles for *N. crassa* showed similar interconversion of alanine and glutamate (Kanamori et al., 1982).

A more novel feature of our $^{15}N$ NMR study is the arginine catabolism in *M. thermoautotrophicum*. There are four known pathways for arginine catabolism (Scheme II): (a) the arginase pathway in which arginine is cleaved to ornithine with elimination of the guanidino group in the form of urea; (b) the arginine dihydrolase pathway in which arginine is converted to citrulline and ammonia; (c) the hydroxylase pathway in which arginine is decarboxylated and converted to $\gamma$-guanidinobutyramide; (d) a transaminase pathway in which arginine is converted to $\alpha$-ketoarginine, decarboxylated to $\gamma$-guanidinobutyraldehyde, oxidized to $\gamma$-guanidinobutyrate, and hydrolyzed to $\gamma$-aminobutyrate. Our $^{15}N$ NMR analysis of the specific labeling of arginine and similar basic species shows that the guanidino group remains intact, thus ruling out the urea cycle (a) and the dihydrolase pathway (b). Both these pathways would lead to new side-chain nitrogen resonances with significantly different chemical shifts, while still retaining the $\alpha$-amino resonance around −335 ppm. Pathways c and d leave the guanidino group intact, but in the case of pathway c, the resonance from a labeled amide group should appear around −270 ppm, which was not observed. The transamination pathway d, however, removes the $\alpha$-amino nitrogen from arginine. Thus, in early stationary (36 h) or stationary-phase (60 h) cells, catabolism of arginine is initiated by transamination, leaving the guanidino group intact and producing $\alpha$-ketoarginine or $\gamma$-guanidinobutyrate as is the case for *Pseudomonas putida* (Vanderbilt et al., 1975). An NMR distinction between these various guanidino species cannot be made, since it was found that the $^{15}N$ chemical shifts of the $\omega,\omega'$ and $\delta$ nitrogens in $\gamma$-guanidinobutyrate were exactly the same as those for arginine, and therefore presumably for $\alpha$-ketoarginine.

The power and utility of $^{15}N$ NMR spectroscopy in defining nitrogen assimilation reactions in novel or unusual microorganisms is now clearly established. Unlike radioactive tracer experiments, an $^{15}N$ NMR analysis provides a rapid method for determining the fate of nitrogen into all possible metabolites as well as specific sites of incorporation. Such versatility should make $^{15}N$ NMR spectroscopy the method of choice for future studies of nitrogen metabolism.

## ACKNOWLEDGMENTS

We thank Prof. William W. Bachovchin (Tufts University Medical School) for the use of his Bruker AM-400 WB NMR spectrometer for high-resolution studies and Dr. Robert G. Griffin (Francis Bitter National Magnet Laboratory) for access to his CP-MASS NMR spectrometer.

**Registry No.** L-Glutamic acid, 56-86-0; L-alanine, 56-41-7; L-arginine, 74-79-3.

## REFERENCES

Daniels, L., Sparling, R., & Sprott, G. D. (1984) *Biochim. Biophys. Acta 768*, 113–163.

Evans, J. N. S., Tolman, C. J., Kanodia, S., & Roberts, M. F. (1985) *Biochemistry 24*, 5693–5698.

Fuchs, G., Stupperich, E., & Thauer, R. K. (1978) *Arch. Microbiol. 117*, 61–66.

Haran, N., Kahana, Z. E., & Lapidot, A. (1983) *J. Biol. Chem. 258*, 12929–12933.

Jacob, G. S., Schaefer, J., Stejskal, E. O., & McKay, R. A. (1980) *Biochem. Biophys. Res. Commun. 88*, 274–280.

Jacob, G. S., Schaefer, J., & Wilson, G. E., Jr. (1983) *J. Biol. Chem. 258*, 10824–10826.

Jacob, G. S., Schaefer, J., & Wilson, G. E., Jr. (1985) *J. Biol. Chem. 260*, 2777–2781.
Kanamori, K., Legerton, T. L., Weiss, R. L., & Roberts, J. D. (1982) *J. Biol. Chem. 257*, 14168–14172.
Kandler, O. (1979) *Naturwissenschaften 66*, 95–105.
Kanodia, S., & Roberts. M. F. (1983) *Proc. Natl. Acad. Sci. U.S.A. 80*, 5217–5221.
Kenealy, W. R., Thompson, T. E., Schubert, K. R., & Zeikus, J. G. (1982) *J. Bacteriol. 150*, 1357–1365.
König, H., & Kandler, O. (1979a) *Arch. Microbiol. 121*, 271–275.
König, H., & Kandler, O. (1979b) *Arch. Microbiol. 123*, 295–299.
Lapidot, A., & Irving, C. S. (1977) *Proc. Natl. Acad. Sci. U.S.A. 74*, 1988–1992.
Lapidot, A., & Irving, C. S. (1979) *Biochemistry 18*, 1788–1796.
Legerton, T. L., Kanamori, K., Weiss, R. L., & Roberts, J. D. (1981) *Proc. Natl. Acad. Sci. U.S.A. 78*, 1495–1498.
Meeks, J. C., Wolk, C. P., Lockau, W., Schilling, N., Shaffer, P. W., & Chien, W. S. (1978) *J. Bacteriol. 134*, 125–130.
Schaefer, J., Skokut, T. A., Stejskal, E. O., McKay, R. A., & Varner, J. E. (1981a) *Proc. Natl. Acad. Sci. U.S.A. 78*, 5978–5982.
Schaefer, J., Skokut, T. A., Stejskal, E. O., McKay, R. A., & Varner, J. E. (1981b) *J. Biol. Chem. 256*, 11574–11579.
Schubert, K. R., & Coker, G. T. III (1981) *Plant Physiol. 67*, 662–665.
Seeley, R. J., & Fahrney, D. E. (1983) *J. Biol. Chem. 258*, 10835–10838.
Stupperich, E., & Fuchs, G. (1981) *Arch. Microbiol. 130*, 294–300.
Stupperich, E., & Fuchs, G. (1984) *Arch. Microbiol. 139*, 8–20.
Taylor, C. T., Kelly, D. P., & Pirt, S. J. (1976) in *Proceedings of the Symposium on Microbial Production and Utilization of Gases ($H_2$, $CH_4$, CO)* (Schlegal, H. G., Gottschalk, G., & Pfenning, N., Eds.) pp 173–180, Akademie der Wissenschaften Zu Göttingen, E. Goltze, Göttingen.
Tyler, B. (1978) *Annu. Rev. Biochem. 47*, 1127–1162.
Vanderbilt, A. S., Gaby, N. S., & Rodwell, V. W. (1975) *J. Biol. Chem. 250*, 5322–5329.
Winters, J. C., & Kunin, R. (1949) *Ind. Eng. Chem. 41*, 460–463.
Zeikus, J. G. (1977) *Bacteriol. Rev. 41*, 514–541.
Zeikus, J. G., Fuchs, C. T., Kenealy, W. R., & Thauer, R. K. (1977) *J. Bacteriol. 132*, 604–613.

# Proliferation Dependence of Topoisomerase II Mediated Drug Action†

Daniel M. Sullivan,‡ Bonnie S. Glisson,‡,§ Paula K. Hodges,§ Sherin Smallwood-Kentro,§ and Warren E. Ross*,‡,§
*Departments of Medicine and Pharmacology, College of Medicine, University of Florida, Gainesville, Florida 32610*
*Received September 4, 1985*

ABSTRACT: Topoisomerase II mediated DNA scission induced by both a nonintercalating agent [4′-demethylepipodophyllotoxin 4-(4,6-*O*-ethylidene-β-D-glucopyranoside) (VP-16)] and an intercalator [4′-(9-acridinylamino)methanesulfon-*m*-anisidide (*m*-AMSA)] was studied as a function of proliferation in Chinese hamster ovary (CHO), HeLa, and mouse leukemia L1210 cell lines. Log-phase CHO cells exhibited dose-dependent drug-induced DNA breaks, while plateau cells were found to be resistant to the effects of VP-16 and *m*-AMSA. Neither decreased viability nor altered drug uptake accounted for the drug resistance of these confluent cells. In contrast to CHO cells, plateau-phase HeLa and L1210 cells remained sensitive to VP-16 and *m*-AMSA. Recovery of drug sensitivity by plateau-phase CHO cells was found to reach a maximum approximately 18 h after these cells regained exponential growth and was independent of DNA synthesis. DNA strand break frequency correlated with cytotoxicity in CHO cells; log cells demonstrated an inverse log linear relationship between drug dose (or DNA damage) and colony survival, whereas plateau-derived colony survival was virtually unaffected by increasing drug dose. Topoisomerase II activity, whether determined by decatenation of kinetoplast DNA, by cleavage of pBR322 DNA, or by precipitation of the DNA–topoisomerase II complex, was uniformly severalfold greater in log-phase CHO cells compared to plateau-phase cells.

DNA topoisomerase II [EC 5.99.1.3; for a review, see Gellert (1981), Liu (1983), and Wang (1985)] is present in both eukaryotes and prokaryotes and exists as a dimer with a subunit molecular mass of 131–180 kilodaltons (kDa),[1] requires magnesium cations and ATP for activity, shows DNA-stimulated ATP hydrolysis, requires the presence of a sulfhydryl reagent for full activity, and changes linking numbers of DNA in steps of two. This enzyme catalyzes DNA topoform interconversions by introducing a transient enzyme-bridged, double-stand break in one of the two crossing

† This work was supported in part by National Institutes of Health Grant CA-24586.
* Address correspondence to this author at the Department of Pharmacology, University of Florida.
‡ Department of Medicine.
§ Department of Pharmacology.

[1] Abbreviations: VP-16, 4′-demethylepipodophyllotoxin 4-(4,6-*O*-ethylidene-β-D-glucopyranoside); *m*-AMSA, 4′-(9-acridinylamino)-methanesulfon-*m*-anisidide; CHO, Chinese hamster ovary; PMSF, phenylmethanesulfonyl fluoride; SDS, sodium dodecyl sulfate; EDTA, ethylenediaminetetraacetic acid; BSA, bovine serum albumin; DTT, dithiothreitol; PBS, phosphate-buffered saline; Tris, tris(hydroxymethyl)-aminomethane; kDa, kilodalton(s).

0006-2960/86/0425-2248$01.50/0 